Smart Agricultural Technology 12 (2025) 101587

Contents lists available at ScienceDirect

Smart Agricultural Technology

journal homepage: www.journals.elsevier.com/smart-agricultural-technology

Potential of thermal imaging for yield and soil water content prediction in leafy vegetables

Vinícius Villa e Vila [a,*], Silas Alves Souza [a], Fernando Campos Mendonça [a], Tamara Maria Gomes [b], Peterson Ricardo Fiorio [a], Patricia Angélica Alves Marques [a]

[a] University of São Paulo/USP, Luiz de Queiroz College of Agriculture/ESALQ, Biosystems Engineering Department, Padua Dias Avenue 11, 13418-900, Piracicaba, SP, Brazil

[b] University of São Paulo/USP, Faculty of Animal Science and Food Engineering/FZEA, Biosystems Engineering Department, Duque de Caxias 225, 13635-900, Pirassununga, SP, Brazil

ARTICLE INFO

Keywords:
Agricultural instrumentation
Canopy temperature
Thermal camera
Water management

ABSTRACT

In agriculture, water deficit stress is among the main causes of crop yield losses, particularly in leafy vegetables, which are highly sensitive. The need for efficient irrigation management and the early identification of potential yield gaps encourage the development of predictive models and the integration of more precise technologies. From this perspective, infrared radiation cameras in the capture of thermal information have potential for application. The objective of this study was to develop predictive models of yield and soil water content in leafy vegetables crops, specifically lettuce and arugula, by integrating thermal images obtained using infrared radiation cameras. Two experiments were carried out in Piracicaba, São Paulo, Brazil, using lettuce and arugula crops, each with two growing cycles. A randomized complete block design (RCBD) was adopted, with three irrigation levels: 100, 80, and 60 % of crop evapotranspiration replacement. For model development, crop yield was assessed based on shoot biomass at harvest, and soil water content was measured using tensiometry-based sensors. The Crop Water Stress Index (CWSI) and the normalized temperature difference (ΔT) were calculated from thermal images of the plant canopy. Yield prediction models exhibited R2 values of 0.71 and 0.82 using CWSI, and 0.75 and 0.79 using ΔT, for lettuce and arugula, respectively, with a mean RMSE of 4.87 t ha-1. Soil water content prediction models showed R2 values of 0.92 based on CWSI and 0.73 based on ΔT, with a mean RMSE of 0.00428 m3 m-3. The developed models demonstrated good predictive performance, indicating their applicability for irrigation management and for predicting possible early yield gaps in leafy vegetables. CWSI and ΔT values above 0.35 and -0.96 °C, respectively, are recommended as critical thresholds to avoid water deficit stress in lettuce and arugula crops.

1. Introduction

Despite the ongoing development of the agricultural sector, one of the major challenges in agriculture remains achieving high crop yields under adverse climatic conditions. It is estimated that potential crop yields may be reduced by up to 70 % due to abiotic stresses, depending on their level and intensity [1–3]. Water and heat stress are among the main factors responsible for yield reductions and may be exacerbated by the impacts of climate change. In addition to these challenges, the increasing global demand for food and the limitation of natural resources require the improvement and adoption of new technologies to optimize agricultural practices and support mitigation strategies.

Water stress can be characterized by changes in plant behavior due to water availability either above or below the crop's physiological requirements. Under water stress conditions, plants experience impairments in essential physiological processes [4], resulting in reduced biomass accumulation and productivity. When soil water availability is limited, the reduction of transpiration becomes a strategy adopted by plants to minimize water loss and ensure survival, as the transpiration process is fundamental in regulating leaf temperature. There is a relationship between water stress and ambient temperature, where increases in temperature can lead to decreased soil moisture due to enhanced soil evaporation. This may intensify water stress by lowering leaf relative water content, ultimately reducing water use efficiency in

* Corresponding author.
E-mail address: viniciusvilla@usp.br (V. Villa e Vila).

https://doi.org/10.1016/j.atech.2025.101587
Received 23 September 2025; Received in revised form 14 October 2025; Accepted 30 October 2025
Available online 31 October 2025

plants [5].

Among the main agricultural crops, leafy vegetables such as lettuce (*Lactuca sativa* L.) and arugula (*Eruca sativa* L.) hold significant importance in human nutrition, with large-scale production and consumption. Global production of major leafy vegetables increased by 69 % between 2000 and 2021 [6]. A challenge in cultivating leafy vegetables is their high sensitivity to water deficit, where soil water availability is a critical factor affecting the development and productivity of these crops [4]. The large leaf area of these plants promotes intense transpiration, increasing water loss to the environment. Additionally, they have a superficial root system and poorly lignified tissues, making them more vulnerable to stress caused by water deficit compared to other crops [6]. Consequently, leafy vegetables are highly dependent on irrigation, requiring constant soil water replacement.

To mitigate these negative impacts, it is essential to adopt efficient water management strategies. Therefore, it is necessary to implement approaches that determine the appropriate timing and amount of water to address crop water requirements, which can be based on climate, soil, and/or plant information. However, traditional irrigation management strategies still present limitations in obtaining this information, as some involve lengthy analysis periods, destructive sampling, and provide only point measurements, such as the direct method for determining soil moisture by gravimetry, which requires taking soil samples from the field and a prolonged drying process. Other strategies require many sensors that are costly and need calibration through direct measurements, such as the use of Time Domain Reflectometry (TDR) and Frequency Domain Reflectometry (FDR) sensors to determine soil moisture [7]. Another way to overcome yield gaps due to water deficit is through early stress detection and yield prediction. In this context, the use of thermal images captured by infrared radiation cameras has gained significant attention due to their ability to provide real-time assessments of plant water status [8].

In agriculture, there are predictive models that use data provided by sensors or direct measurements integrated with agronomic characteristics related to plant morphology and physiology [3,9]. Among these, the integration of predictive models with thermal images has gained prominence. Besides being commonly used for water stress detection, thermal imaging also has potential for predicting yield and soil water content, thereby assisting irrigation management [10]. However, some models used for this purpose are complex and require a large quantity and variety of data, which are often difficult to obtain, making their practical application less accessible to farmers. Employing less complex models, particularly those informed by accurate and dependable data from infrared cameras, can improve the accessibility of this approach and increase its potential for agricultural applications.

Infrared cameras are sensors that measure radiation emitted by target objects within the infrared wavelength range and convert it into thermal images. These images provide the temperature distribution of the objects across different temperature gradients. Canopy temperature is an indicator of crop water stress [11–13]. The detection of temperature to assess water stress depends on the plant's transpiration process. Under water deficit conditions, stomatal closure occurs, resulting in reduced water vapor release to the atmosphere. Consequently, leaf temperature increases due to the decreased cooling capacity of the leaves [14–16]. Compared to traditional methods, thermal imaging can capture large-scale spatial variability across the entire field, rather than just at specific points [17]. In addition, it enables rapid and non-destructive identification with lower labor requirements [9,18–20], offering a comprehensive understanding of soil–plant–atmosphere interactions.

Canopy temperature alone is not considered an efficient indicator of water stress [21]. Therefore, water stress can be characterized through thermal indices, such as the normalized temperature difference (ΔT) and the Crop Water Stress Index (CWSI) [22,23]. ΔT is obtained by calculating the difference between canopy temperature and air temperature, while CWSI is a more robust index that, in addition to comparing canopy and air temperatures, also incorporates reference values for well-irrigated and severely stressed plants [24,25]. Among these, CWSI is the most commonly used index for stress detection, as it overcomes the influence of other environmental parameters that affect plant temperature [3]. However, the practical application of this index is still limited, mainly due to the complexity of data acquisition and associated costs. Nevertheless, there are mobile applications capable of calculating CWSI based on temporal parameters using empirical and theoretical models, which reduce their complexity [26], Additionally, infrared thermographic cameras with lower acquisition costs, depending on their embedded technology level, are becoming more available, improving the accessibility of this approach for farmers [27,28].

Recent literature demonstrates the frequent use of thermal imaging as a diagnostic tool for water stress in agricultural crops. In this context, research has been conducted in wheat [3,10,20,29], soybean [30], maize [11,21], citrus [27,31], grapevine [32–34], sugar beet [35] and turfgrass [16]. Some studies have examined correlations between thermal data and yield or soil water parameters, revealing strong associations and demonstrating the potential for developing predictive models. For example, Ma [20] observed correlations between the CWSI, biomass, and yield in wheat under different water conditions and phenological stages. Similarly, Morales-Santos and Nolz [30] found correlations between various thermal indices and soil water potential in soybean at different depths (0.20, 0.40, and 0.60 m).

While the use of thermal imaging is analyzed in grain and fruit crops, its application in leafy vegetables remains largely unexplored and requires further research. In addition to the applications found in the highlighted studies, further detail of these parameters is still required in irrigation management. These studies associate thermal information with qualitative aspects of irrigation management, relying on other strategies and information to be applicable in the field. Therefore, studies integrating soil moisture information with thermal indices in a quantitative manner are needed to support irrigation management decisions.

Considering the importance of thermal information and its relationship with crop yield and soil water dynamics, this study hypothesized that it is possible to develop predictive models by integrating thermal image data to provide assessments of water stress, soil water content, and crop yield. These models can assist in irrigation management and early detection of yield gaps, especially in leafy vegetables, which have short production cycles and are highly sensitive to water deficit stress. The objective of this study was to develop predictive models, based on regression and correlation analysis, for yield and soil water content in the cultivation of leafy vegetables, specifically lettuce and arugula, by integrating thermal images obtained from infrared radiation cameras.

2. Material and methods

2.1. Experimental area

The study was conducted in a protected environment at the experimental area of the Department of Biosystems Engineering, "Luiz de Queiroz" College of Agriculture (ESALQ), belonging to the University of São Paulo (USP), in Piracicaba, São Paulo, Brazil (22°42′32″ S, 47°37′45″ W, 546 m of altitude).

The regional climate, according to the Köppen classification, is characterized as a humid subtropical zone (Cwa), with hot and humid summers and dry winters. The region has an average annual precipitation of 1280 mm, a mean air temperature of 21.6 °C, an average relative humidity of 73 % [36] and a mean maximum reference evapotranspiration of approximately 5.78 mm dia^{-1} [37].

The local soil is classified as Red-Yellow Latosol [38], with a clayey texture. The physical (Clay, silt and sand) and hydro-physical (Bd, θ_{FC}, θ_{PWP} and AWC) soil properties as well as the chemical soil parameters for the two cropping cycles, corresponding to the 0–0.20 m layer, are

presented in Tables 1 and 2, respectively.

2.2. Experiment setup and management

In this study, two simultaneous experiments were conducted with leafy vegetables: one with lettuce (Experiment 1) and another with arugula (Experiment 2). The plants were grown in a protected environment to ensure greater experimental control and data reliability, while minimizing external climatic influences. The structure was covered with 150 μm thick transparent light-diffusing plastic and had lateral protection made of 50 MESH aphid-proof screens, manufactured from polyethylene allowing air exchange with the environment. The structure presented a ceiling height of 4 m and dimensions of 20 m in length and 10 m in width.

To initiate the experiments, soil tillage was performed to prepare the cultivation beds. Each bed measured 1.25 m in length, 0.4 m in width, and 0.2 m in height, resulting in an effective area of 0.5 m^2. A spacing of 1 m was left between beds to prevent water flow from one bed to another, since irrigated cultivation was carried out. At the time of bed construction, 25 L of well-composted cattle manure were incorporated per bed, with a composition of 336 kg ha^{-1} N, 125 kg ha^{-1} P_2O_5, 113 kg ha^{-1} K_2O, 136 kg ha^{-1} Ca and 42 kg ha^{-1} Mg. In addition, mineral fertilization at planting was carried out by applying 40 kg ha^{-1} N, 300 kg ha^{-1} P_2O_5 and 150 kg ha^{-1} K_2O per bed. All fertilization recommendations were made according to Van Raij [39], based on the soil chemical analysis (Table 2).

Each experiment was conducted over two cropping cycles. The first cycle lasted from May 30, 2022, to July 9, 2022, and the second from July 19, 2022, to August 28, 2022, with each cycle lasting 40 days. In Experiment 1, the lettuce cultivar Vanda® was used, characterized as a crisphead type with high hardiness and adaptability to various growing conditions, and it is the most widely planted cultivar in Brazil. Lettuce was sown in polyethylene trays, and seedlings were transplanted to the beds 25 days after sowing (DAS). Lettuce was grown in double rows, spaced 0.20 m between rows and 0.30 m between plants, totaling 8 plants per bed. During the lettuce cultivation, three topdressings via fertigation were performed, applying 25 kg ha^{-1} of N at 10, 20, and 30 days after transplanting (DAT). In Experiment 2, the arugula cultivar Astro® was used, characterized by broad leaves and less lobed shape, with high tolerance to premature bolting. Arugula was sown directly in the soil in double rows, using a higher density than recommended for the crop to allow for subsequent thinning of seedlings. After the emergence of two true leaves, excess seedlings were thinned, resulting in 100 plants per bed, spaced 0.20 m between rows and 0.025 m between plants. During arugula cultivation, three topdressings via fertigation were applied, with 40 kg ha^{-1} of N at 10, 17, and 24 DAS.

2.3. Experimental design

The experiments were conducted using a randomized complete block design (RCBD). Lettuce and arugula plants were subjected to three treatments, corresponding to different water replacement levels relative to crop evapotranspiration (ETc): 100, 80, and 60 % of ETc. These conditions represent optimal water availability without water stress (100 % ETc), moderate water deficit (80 % ETc), and severe water deficit (60 % ETc). Each treatment consisted of five replications, with each bed considered as an experimental unit.

Table 1
Physical and hydro-physical soil properties in the 0–0.20 m layer.

Bd	θ_{FC}	θ_{PWP}	AWC	Clay	Silt	Sand
g cm^{-3}	m^3 m^{-3}		mm	%		
1.28	0.41	0.28	26.00	54.93	15.26	29.81

Bd: bulk density; θ_{FC}: moisture at field capacity; θ_{PWP}: moisture at permanent wilting point; AWC: available water capacity.

Table 2
Chemical soil parameters in the 0–0.20 m layer.

Cycle	pH $CaCl_2$	Ca	Mg	K	H	Al	CEC	V
	-	mmolc dm^{-3}						%
First	5.8	53.0	21.0	7.8	14.0	0.0	95.8	85.4
Second	5.6	65.0	21.0	8.2	16.0	0.0	110.2	85.5
	OC	P resin	S	B	Cu	Zn	Mn	Fe
	g dm^{-3}	mg dm^{-3}						
First	26.0	69.0	25.7	0.2	1.2	2.7	8.1	9.0
Second	23.0	70.0	24.8	0.2	1.5	2.6	9.5	8.0

OC: Organic carbon; CEC: cation exchange capacity; V: base saturation.

2.4. Irrigation system and management

A drip irrigation system was installed in the protected environment. Each experimental unit contained a 1.25 m long drip line positioned at the center, with an independent irrigation system and valves installed at the beginning of each bed to allow precise control of the different water replacement treatments. The drip tape had a diameter of 0.016 m, with emitters spaced every 0.20 m, totaling seven emitters per line. The emitters, featuring pressure-compensating and anti-siphon characteristics, had a flow rate of 1.6 L h^{-1} each, resulting in a total flow rate of 11.2 L h^{-1}. The system was operated by a KSB 500 N motor pump at a working pressure of 1.0 bar. Irrigation uniformity was evaluated by calculating the Christiansen Uniformity Coefficient (CUC), obtaining a value of 98.5 %, indicating a high level of uniformity.

Inside the protected environment, a meteorological station was installed to monitor climatic variables during the experiments. The station was equipped with air temperature and relative humidity sensors (HMP45C), a solar radiation sensor (LI200X), and a barometer (CS106), with readings taken every 15 min, connected to a CR23X datalogger (Campbell Scientific, Logan, Utah, USA).

Irrigation management was performed using climate-based method to determine the water demand for each irrigation event. ETc was estimated according to the methodology proposed by FAO 56, calculated using Eq. (1). Reference evapotranspiration (ETo) was estimated following the Penman-Monteith equation (Eq. (2)). The crop coefficient (Kc) values used for lettuce were 0.70, 1.00, and 0.95, while for arugula they were 0.80, 1.00, and 1.05, corresponding to the initial, intermediate, and final growth stages, respectively, also according to FAO 56 [40].

$$ETc = ETo\ Kc \tag{1}$$

where ETc is the crop evapotranspiration (mm day^{-1}), ETo is the reference evapotranspiration (mm day^{-1}), and Kc is the crop coefficient (dimensionless).

$$ETo = \frac{0.408\ \Delta\ (Rn\ -\ G) + \gamma\left(\frac{900}{T\ +\ 273}\right)\ u2\ (es\ -ea)}{\Delta\ +\ \gamma\ (1\ +\ 0.34\ u2)} \tag{2}$$

where Rn is the surface radiation balance (MJ m^{-2} $_D$ $^{-1}$), G is the soil heat flux density (MJ m^{-2} $_D$ $^{-1}$), T is the air temperature at 2 m height (°C), u2 is the wind speed at 2 m height (m s^{-1}), es is the saturation vapour pressure (kPa), ea is the partial vapour pressure (kPa), Δ is the slope of the saturation vapour pressure curve (kPa °C^{-1}) and γ is the psychrometric constant (kPa °C^{-1}).

The irrigation depth (ID) for each treatment was calculated using Eqs. (3),4, and 5, considering a system application efficiency (Ea) of 95 %. Irrigations were performed with daily irrigation shifts at 8:00 a.m.

$$ID_{100} = \frac{ETc}{Ea} \tag{3}$$

$$ID_{80} = (ID_{100})\ 0.80 \tag{4}$$

$$ID_{60} = (ID_{100})\ 0.60 \tag{5}$$

where ID_{100} is the irrigation depth for 100 % ETc replacement (mm), ID_{80} is the irrigation depth for 80 % ETc replacement (mm), ID_{60} is the irrigation depth for 60 % ETc replacement (mm), ETc is the crop evapotranspiration (mm day^{-1}), and Ea is the application efficiency (expressed as a decimal).

2.5. Monitoring and assessment of soil water content

To monitor soil water content, tensiometers were installed in all treatments of both experiments and cropping cycles, at the 0–0.20 m soil depth. The tensiometers were installed in three experimental units per treatment, with three replications in each unit, and positioned in the center of the experimental unit, between the two crop rows. Tensiometer is a soil sensor that, through a porous ceramic cup in contact with the soil, enables water exchange between the soil and the tube, creating a vacuum that reflects the tension at which water is retained in the soil. From the soil water potential (-kPa) readings obtained using a digital tensimeter, the soil water content (m^3 m^{-3}) was indirectly determined using the soil water retention curve (Fig. 1).

To obtain the soil moisture points that compose the soil water retention curve, undisturbed soil samples were collected from the 0–0.20 m layer, with three replications. The soil moisture points were determined by subjecting the soil samples to a Richards pressure chamber at pressure heads of 0, –10, –20, –40, –100, –300, –500, –1000, and –1500 kPa, following the procedures described by Camargo [41]. The soil water retention curve was fitted using the Van Genuchten model [42]. The fitted parameters of the soil water retention curve are presented in Table 3.

Soil water potential readings were taken daily to validate the climate-based irrigation management. For the study on the prediction of soil water content using thermal imaging data, the readings collected on the same day as the thermal images were considered. Despite the differences in canopy architecture and leaf morphology between the two leafy vegetables, there is a similarity in the water demand of the crops [40] and due to the comparable behavior of both crops across the two cropping cycles, the predictive model of soil water content was developed by integrating data obtained from both cycles and both crops, to increase the model's reliability.

2.6. Thermal image data acquisition and processing

The sensor used to acquire thermal images of the lettuce and arugula canopies was a FLIR T640 Duo Pro R thermal camera, which operates in the spectral band of 7.5–13.5 μm, with a resolution of 640 × 512 pixels and a thermal sensitivity of <50 mK. Prior to image acquisition, the thermal camera was configured according to the prevailing meteorological conditions at the time of image capture. Additionally, the emissivity (ε) was set to 0.95, in accordance with the spectral signature of the target surface.

One thermal image was acquired for each experimental unit. Image acquisition was standardized in terms of camera positioning distance from the canopy (1.5 m), parallel to the canopy (top view), with acquisition time (between 12:00 and 13:00 local time), and the prevailing meteorological conditions. All images were captured under clear-sky conditions, without cloud cover, when the crops were at the final stage of development (35 DAT), close to harvest. At this stage, the vegetative growth of the crop stabilizes.

Following acquisition, the images were processed using FLIR Thermal Studio® software, version 2.0.11. The images were imported and processed to minimize noise and potential contamination from pixels outside the experimental unit. To increase the precision of the thermal information, each image was cropped to include only the usable area of the experimental unit. The images were then classified using the "iron" color palette, and the temperature scale (minimum and maximum) was standardized. To sample temperature data, a line was drawn parallel to the longest dimension of each image at the center of the experimental unit. Five points were randomly selected along this line to obtain an average canopy temperature, which was subsequently used to calculate other thermal parameters, including ΔT and CWSI. Fig. 2 shows the main steps involved in the acquisition and processing of the thermal images.

Table 3
Soil water retention curve parameters in the 0–0.20 m layer.

θr	θs	α	n	m	R^2
m^3 m^{-3}		m^{-1}	-	-	-
0.128	0.537	1.286	1.101	0.092	0.992

θr: residual water content; θs: saturated water content; α: inverse of the air-entry potential in the structural pore space; n: empirical curve fitting parameter; m: Mualem restriction parameter; R^2: determination coefficient.

2.7. Thermal parameters

The crops water status was characterized using CWSI and ΔT. To calculate the CWSI, two reference limits were required to normalize the effects of atmospheric conditions on canopy transpiration and temperature [24,25]. These limits include the baseline for a non-stressed plant (Twet), representing a well-irrigated crop with no water restrictions, and the baseline for a water-stressed plant (Tdry), indicating a crop with limited or nearly no transpiration due to stomatal closure.

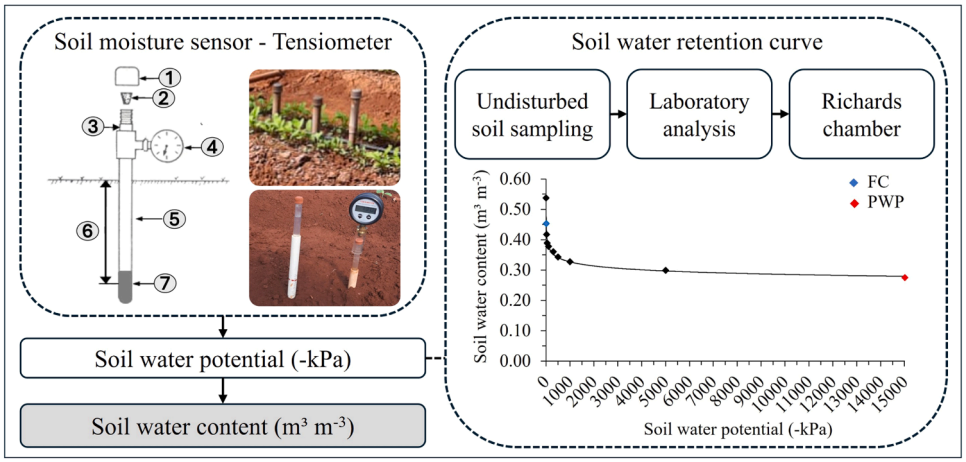

Fig. 1. Flowchart of soil water content determination. Cap (1); rubber stopper (2); acrylic tube (3); tensiometer (4); PVC tube (5); soil moisture monitoring depth (6); and porous cup (7). FC: Field capacity; PWP: Permanent wilting point.

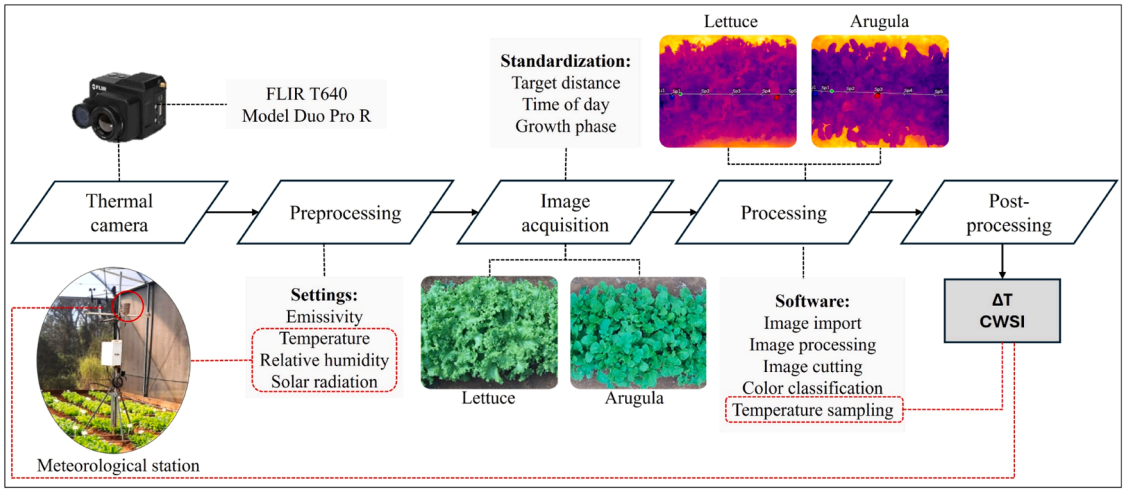

Fig. 2. Flowchart of thermal image acquisition and processing. ΔT: Normalized temperature difference index; CWSI: crop water stress index.

In general, the baseline limits can be determined using an empirical approach [43], through natural wet and dry reference surfaces [44], or under actual field conditions. In this study, the baselines were established based on real field conditions obtained from the experiments. Specifically, thermal image temperature thresholds from the 100 % and 60 % ETc irrigation treatments were used to represent the non-stressed (Twet) and water-stressed (Tdry) conditions, respectively. Therefore, the CWSI was calculated using Eq. (6) [25]. CWSI values can range from zero to one (0–1). A CWSI value of 0 indicates the absence of water stress, while a value of 1 corresponds to maximum water stress.

$$\mathrm{CWSI} = \frac{(\mathrm{Tc} - \mathrm{Ta}) - \mathrm{Twet}}{\mathrm{Tdry} - \mathrm{Twet}} \tag{6}$$

where CWSI is the Crop Water Stress Index (dimensionless), Tc is the canopy temperature (°C), Ta is the air temperature at the time of Tc acquisition (°C), Twet is the baseline canopy temperature of a non-stressed plant (°C), and Tdry is the baseline canopy temperature of a water-stressed plant (°C).

The ΔT was calculated using Eq. (7). ΔT values can be negative, zero, or positive. A negative ΔT value indicates the absence of water stress, while a positive value corresponds to the presence of water stress.

$$\Delta T = \mathrm{Tc} - \mathrm{Ta} \tag{7}$$

where ΔT is the normalized temperature difference (°C), Tc is the canopy temperature (°C), and Ta is the air temperature at the time of Tc acquisition (°C).

Based on the critical soil water potential of −20 kPa for leafy vegetables, as established by Marouelli [45], the generated models identified the critical limits of CWSI and ΔT, considering both leafy vegetables.

2.8. Crop yields of lettuce and arugula

In both cropping cycles of the two analyzed crops, the cycle duration was 40 days. Yield was measured by obtaining the fresh mass of the aerial parts, consisting only of leaves and stems. Plants were cut at soil level and weighed using an analytical balance (precision 0.001 g). Yield was extrapolated to t ha^{-1}, considering the amount produced in each experimental unit.

2.9. Statistical analysis and models evaluation

To analyze data behavior and variability, descriptive statistical analysis was performed. To develop the prediction models for yield and soil water content, regression and correlation analysis was conducted between these variables and both CWSI and ΔT. Model performance was evaluated using the following statistical indicators: root mean square error (RMSE), mean absolute error (MAE), Nash–Sutcliffe efficiency (NSE), Willmott's index of agreement (d), Pearson correlation coefficient (r), and confidence index (c). The statistical indicators were calculated using Eqs. (8) to 13, respectively. All statistical indicators were performed based on the individual observed (O_i) and predicted (P_i) values, and their respective means ($\bar{O}$ and $\bar{P}$), and the number of data points (N).

$$\mathrm{RMSE} = \sqrt{\frac{\Sigma\,(P_i - O_i)^2}{N}} \tag{8}$$

$$\mathrm{MAE} = \frac{\Sigma\,|P_i - O_i|}{N} \tag{9}$$

$$\mathrm{NSE} = 1 - \left[\frac{\Sigma\,(O_i - P_i)^2}{\Sigma\,(O_i - \overline{O})^2}\right] \tag{10}$$

$$d = 1 - \left[\frac{\Sigma\,(P_i - O_i)^2}{\Sigma\,(|P_i - \overline{O}| + |O_i - \overline{O}|)^2}\right] \tag{11}$$

$$r = \frac{\Sigma\,(P_i - P)(O_i - \overline{O})}{\sqrt{\Sigma\,(P_i - P)^2\,(\Sigma\,O_i - \overline{O})^2}} \tag{12}$$

$$C = r\,d \tag{13}$$

An RMSE below 10 % is classified as perfect, between 10 % and 20 % as good, between 20 % and 30 % as acceptable, and above 30 % as poor. NSE values between 0 and 1 are considered acceptable levels of performance, with values closer to 1 indicating better model performance, whereas values below 0 indicate unacceptable performance [46]. For the "d" index, values close to 1 indicate acceptable performance, whereas values near 0 indicate poor model performance [47]. The r values were interpreted according to the classification proposed by

Table 4
Classification of Pearson correlation coefficient (r) values.

Pearson correlation coefficient (r)	Classification
0.0 - 0.1	**Very low**
0.1 - 0.3	**Low**
0.3 - 0.5	**Moderate**
0.5 - 0.7	**High**
0.7 - 0.9	**Very high**
0.9 - 1.0	**Nearly perfect**

Hopkins [48] (Table 4). The classification of the "c" index followed the interpretation criteria presented in Table 5 [49].

3. Results and discussion

3.1. Meteorological conditions

The observed temperature and solar radiation values during the two cycles of lettuce and arugula are presented in Fig. 3. In the first cycle (Fig. 3A), the maximum temperature ranged from 23.2 to 36.4 °C, reaching its maximum value at 34 DAS, when the plants were in an advanced vegetative growth phenological stage. The minimum temperature varied from 5.6 to 17.6 °C, with the lowest temperature recorded at 14 DAS, during the initial vegetative development stage. The average maximum and minimum temperatures were 31.8 °C and 12.3 °C, respectively, resulting in a mean temperature of 22 °C. Solar radiation ranged from 3.0 to 11.6 MJ m^{-2} day^{-1}, with a mean value of 9.31 MJ m^{-2} day^{-1}.

In the second cycle (Fig. 3B), the maximum temperature ranged from 18.9 to 37.3 °C, with the highest value recorded at 15 DAS. The minimum temperature varied from 6.8 to 17.1 °C, with the lowest temperature observed at 12 DAS. Both the highest and lowest temperature events occurred when the crops were in the initial vegetative development stage. The average maximum and minimum temperatures were 32.1 °C and 12.7 °C, respectively, resulting in a mean temperature of 24.1 °C. Solar radiation ranged from 2.6 to 12.9 MJ m^{-2} day^{-1}, with a mean value of 9.3 MJ m^{-2} day^{-1}.

Vegetable cultivation is influenced by meteorological conditions, which directly impact plant growth and development, as well as product quality. These crops possess physiological characteristics that make them sensitive to significant climatic variations, especially under the influence of climate change [50,51]. Many of these vegetables originate from temperate climate regions and are adapted to moderate temperatures, experiencing difficulties developing under high-temperature conditions [52].

Under adverse climatic conditions, which can cause various physiological disorders, cultivation in protected environments can favor proper crop development [53]. However, very low temperatures may reduce photosynthetic rates and delay vegetative growth. Conversely, high solar radiation can increase leaf temperature and induce stress in plants [54,55]. In both cultivation cycles, the average air temperature and solar radiation values were adequate for growing leafy vegetables.

The ETc for lettuce and arugula in both cultivation cycles is presented in Fig. 4. The total water demand for lettuce was 120.1 and 122.4 mm, while for arugula it was 124.4 and 126.4 mm for the first and second cycles, respectively. In the first cycle (Fig. 4A), ETc ranged from 0.64 to 3.99 mm day^{-1} for lettuce and from 0.74 to 4.04 mm day^{-1} for arugula cultivation. In the second cycle (Fig. 4B), ETc ranged from 0.90 to 4.50 mm day^{-1} for lettuce and from 0.90 to 4.81 mm day^{-1} for arugula cultivation, both considering the 100 % ETc irrigation condition, with proportional reductions for the deficit irrigation levels (80 and 60 % of ETc).

Although the arugula crop exhibited a higher water demand compared to lettuce, the average ETc values for both vegetables were similar. In the first cycle, these values were 2.93 mm day^{-1} for lettuce and 3.03 mm day^{-1} for arugula, while in the second cycle the values were 2.99 mm day^{-1} and 3.08 mm day^{-1}, respectively. Comparing the water demands across different cycles also showed similarity, with a slight increase in the second cycle. Evapotranspiration values are influenced by climatic variables during the experimental periods, mainly solar radiation, air temperature, and relative humidity [56].

Periods with intense solar radiation and higher air temperatures contributed to higher ETc values, as evidenced between June 21 and 24 in the first cycle, and between August 12 and 15 in the second cycle. Additionally, the variation in ETc between cycles is associated not only with the meteorological conditions of the cultivation site but also with the phenological stage of the crops and their production environment [57]. During these periods, the crops were at an advanced vegetative development stage, which corresponds to the phase of highest water demand.

Table 5
Criteria for interpreting the performance of estimation methods by index "c".

Index "c"	Performance
> 0.85	Great
0.76 - 0.85	Very good
0.66 – 0.75	Good
0.61 – 0.65	Median
0.51 – 0.60	Bad
0.41 – 0.50	Very bad
≤ 0.40	Terrible

3.2. Thermal images and canopy temperature parameters

The cultivation of the crops under different irrigation replacement conditions was reflected in distinct canopy temperature values, as identified by the thermal camera (Fig. 5). A similar color tone pattern was observed in the thermal images for each irrigation level, and this behavior was consistent across both crop cycles and for both leafy vegetables. Under the 100 % ETc condition, the images displayed darker tones, indicating lower leaf temperatures. In contrast, under water deficit conditions, the canopy exhibited lighter tones, reflecting an increase in leaf temperature, most pronounced under the 60 % ETc condition and intermediate under the 80 % ETc irrigation replacement.

Table 6 presents the values of canopy temperature, ΔT and CWSI. In the first cycle, the average canopy temperatures of lettuce were 24.84, 26.62, and 27.82 °C, while for arugula, the values were 25.30, 27.40, and 29.42 °C under 100, 80, and 60 % ETc, respectively. This trend of increasing temperature values with decreasing water availability was also observed in the second cultivation cycle for both crops. In the second cycle of lettuce, the average canopy temperatures were 27.04, 30.04, and 30.96 °C, while for arugula, the values were 27.86, 29.96, and 31.10 °C under the 100, 80, and 60 % ETc irrigation levels, respectively.

Considering both cropping cycles, the average canopy temperature for lettuce was 25.94, 28.33, and 29.39 °C, while for arugula it was 26.58, 28.69, and 30.26 °C, under 100, 80, and 60 % ETc, respectively. Compared to the 100 % ETc, canopy temperature in lettuce increased by an average of 2.39 and 3.45 °C under the 80 and 60 % ETc, respectively. For arugula, the increase was 2.11 and 3.68 °C under 80 and 60 % ETc, respectively. Additionally, the average canopy temperatures recorded during the second cycle were higher than those observed in the first cycle. This difference is attributed to the air temperature at the time of thermal image acquisition, which was 26.35 °C in the first and 29.58 °C in the second cycle.

For lettuce, in the first cycle, the average ΔT values were −1.51, 0.27, and 1.47 °C under 100, 80, and 60 % ETc, respectively. In the second cycle, these values were −2.54, 0.46, and 1.38 °C, respectively. For arugula, ΔT values in the first cycle were −1.05, 1.07, and 3.07 °C, and −1.72, 0.38, and 1.52 °C in the second cycle, under 100, 80, and 60 % ETc, respectively. Considering both cycles, the average ΔT values for lettuce were −2.03, 0.37, and 1.43 °C, and for arugula were −1.38, 0.77, and 2.30 °C under 100, 80, and 60 % ETc, respectively. The ΔT was negative under the optimal water replacement condition (100 % ETc). When water availability was reduced (80 % and 60 % ETc), ΔT became positive. These results confirm that plants under 80 % and 60 % ETc were under water stress, as their canopy temperatures exceeded air temperature. Conversely, under 100 % ETc, canopy temperatures were lower than air temperature, indicating the absence of water stress.

Analyzing the mean CWSI values under the three irrigation levels for lettuce, the values were 0.17, 0.61, and 0.91 in the first cycle, and 0.13,

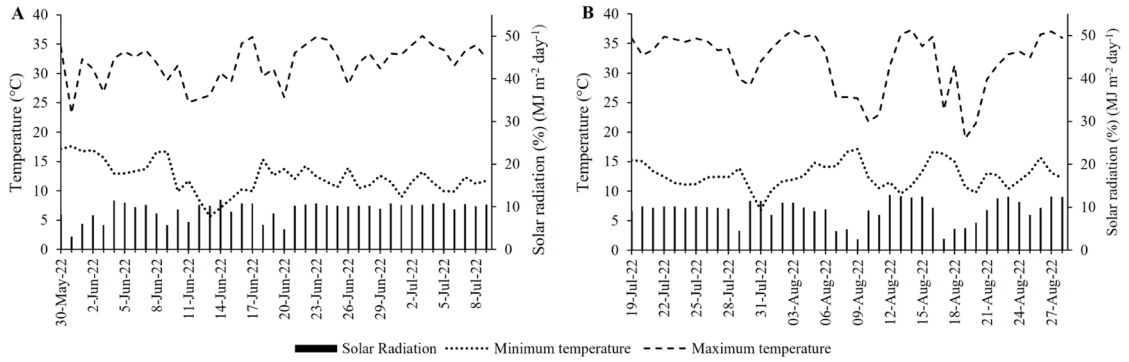

Fig. 3. Values of maximum and minimum temperature (°C) and solar radiation (MJ m^{-2} day^{-1}) observed during the experiment. A) first cycle, and B) second cycle.

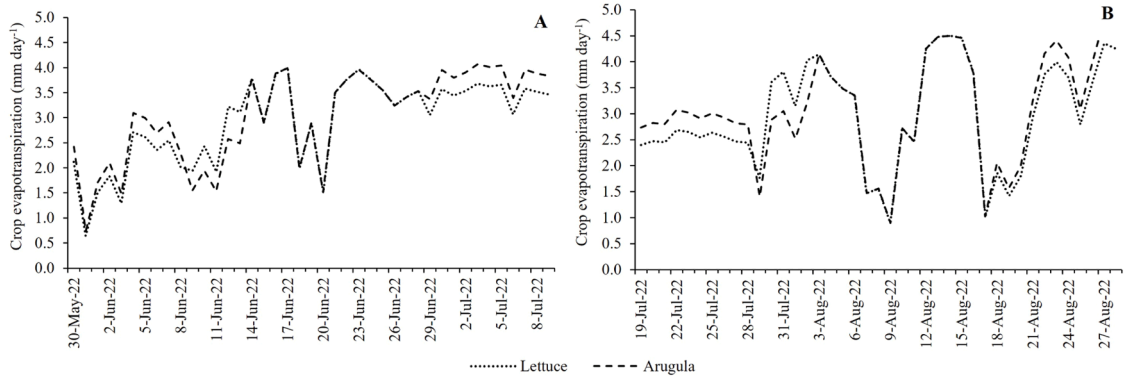

Fig. 4. Values of crop evapotranspiration (mm day^{-1}) during the experiment. A) first cycle, and B) second cycle.

0.69, and 0.85 in the second cycle, for 100, 80, and 60 % ETc, respectively. For arugula, the CWSI values were 0.22, 0.49, and 0.73 in the first cycle, and 0.17, 0.65, and 0.91 in the second cycle, respectively. Considering both cultivation cycles, the average CWSI values for lettuce were 0.15, 0.65, and 0.88, and for arugula were 0.20, 0.57, and 0.82, under 100, 80, and 60 % ETc, respectively.

The results demonstrated that canopy temperature increased as irrigation levels decreased, confirming that water availability directly affects a plant's ability to regulate its temperature through transpiration [14,15]. Plants subjected to water deficit reduce stomatal opening to minimize water loss, which limits evaporative cooling and consequently raises leaf surface temperature [16]. Under higher air temperature conditions, the evapotranspiration demand is greater, but the reduction in water availability impairs the plant's ability to respond effectively, leading to increased canopy temperatures. The relationship between irrigation levels and canopy temperature highlights the importance of appropriate irrigation management to prevent severe water stress, which could compromise both yield and quality of leafy vegetables.

Negative ΔT values under 100 % ETc irrigation indicate that adequately irrigated plants are able to maintain lower leaf temperatures than the surrounding air due to efficient evapotranspiration. When irrigation is insufficient, exposing the plants to water stress, leaf temperature exceeds air temperature. This occurs because transpiration, one of the components of evapotranspiration, is fundamental in maintaining leaf temperature by dissipating heat, thereby preserving metabolic activity and the proper functioning of the photosynthetic apparatus [58].

The CWSI is a reliable parameter for assessing water stress levels in crops, being directly associated with the plant's irrigation status. Higher CWSI values indicate more severe stress caused by water deficit. In both crops and across both growing cycles, CWSI values were higher under water stress conditions, with values approaching 1 at 60 % ETc, and close to 0 under well-watered conditions (100 % ETc). Moreover, CWSI can be used to identify stress thresholds, meaning it is possible to determine a specific CWSI value beyond which the crop begins to experience water stress.

3.3. *Thermal parameters for predicting crop yield*

The yield of the leafy vegetables was influenced by the different irrigation levels (Table 7). Yield reduction was observed as the amount of applied water decreased. For lettuce, in the first cycle, the average yields were 51.76, 44.89, and 29.69 t ha^{-1}, and in the second cycle, 61.82, 48.27, and 41.11 t ha^{-1}, under 100, 80, and 60 % of ETc, respectively. For arugula, in the first cycle, the average yields were 48.24, 34.29, and 23.64 t ha^{-1}, and in the second cycle, 51.15, 32.83, and 27.68 t ha^{-1}, under 100, 80, and 60 % of ETc, respectively. Considering both lettuce growing cycles, the 100 % ETc condition resulted in an average yield of 56.79 t ha^{-1}, which was 17.98 % higher compared to the 80 % ETc treatment and 37.67 % higher than the 60 % ETc treatment. For arugula, across both cycles, the 100 % ETc condition resulted in an average yield of 49.69 t ha^{-1}, representing a 31.96 % increase over the 80 % ETc treatment and 48.36 % over the 60 % ETc treatment.

Water deficit is one of the main factors limiting crop yield, representing a major challenge for sustainable production in the context of climate change and increasing global food demand. As observed, when soil water becomes limited, plants undergo water stress, which can trigger a series of metabolic responses that negatively affect growth and productivity. This condition can also directly impair physiological processes such as photosynthesis, nutrient translocation, and maintenance of cellular turgor [59,60]. The CWSI is a robust index that is strongly correlated with plant physiological indicators. A rise in CWSI is associated with reduced stomatal conductance, which compromises transpiration rate and consequently increases leaf temperature [23].

These physiological mechanisms may have been impaired in both

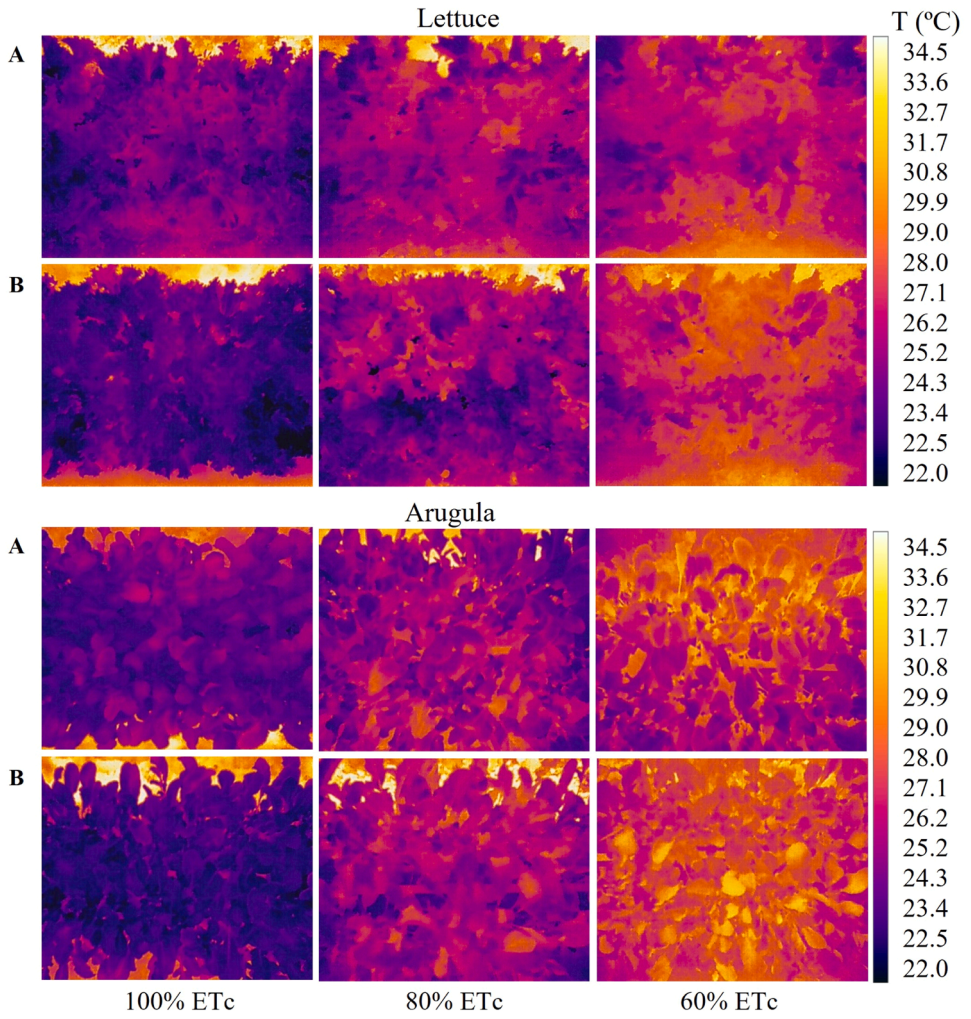

Fig. 5. Canopy thermal images of lettuce and arugula under different water replacement levels. A) first cycle, and B) second cycle.

Table 6
Thermal parameters of lettuce and arugula under different water replacement levels.

Parameters	Water replacement levels (%)	First cycle				Second cycle			
		Max	Min	$\bar{x}$	σ	$\bar{x}$	Min	$\bar{x}$	σ
				Lettuce					
Canopy temperature (°C)	100	25.20	24.30	24.84	0.34	27.50	26.50	27.04	0.36
	80	26.90	26.30	26.62	0.23	30.50	29.00	30.04	0.61
	60	28.10	27.50	27.82	0.26	31.60	29.80	30.96	0.69
ΔT (°C)	100	−2.05	−1.15	−1.51	0.34	−3.08	−2.08	−2.54	0.36
	80	0.55	−0.05	0.27	0.23	0.92	0.52	0.46	0.61
	60	1.75	1.15	1.47	0.26	2.02	0.22	1.38	0.69
CWSI	100	0.24	0.13	0.17	0.04	0.20	0.10	0.13	0.04
	80	0.68	0.53	0.61	0.06	0.78	0.49	0.69	0.12
	60	0.97	0.84	0.91	0.05	0.94	0.65	0.85	0.12
				Arugula					
Canopy temperature (°C)	100	26.31	24.10	25.30	0.81	28.20	27.30	27.86	0.35
	80	28.30	26.60	27.42	0.65	30.40	29.70	29.96	0.32
	60	30.90	28.80	29.42	0.85	31.40	30.70	31.10	0.29
ΔT (°C)	100	−2.25	−0.04	−1.05	0.81	−2.28	−1.38	−1.72	0.35
	80	1.95	0.25	1.07	0.65	0.82	0.12	0.38	0.32
	60	4.55	2.45	3.07	0.85	1.82	1.12	1.52	0.29
CWSI	100	0.33	0.15	0.22	0.07	0.22	0.12	0.17	0.04
	80	0.62	0.37	0.49	0.10	0.76	0.59	0.65	0.08
	60	0.76	0.69	0.73	0.03	0.98	0.83	0.91	0.06

ΔT: Normalized temperature difference (°C); CWSI: Crop Water Stress Index; Max: maximum; Min: minimum; $\bar{x}$: mean; σ: standard deviation.

Table 7
Lettuce and arugula yield under different water replacement levels.

Parameters	Water replacement levels (%)	First cycle				Second cycle			
		Max	Min	$\bar{x}$	σ	Max	Min	$\bar{x}$	σ
					Lettuce				
Yield (t ha^{-1})	100	52.48	50.64	51.75	0.77	68.40	58.32	61.82	3.84
	80	46.24	42.48	44.89	1.75	51.28	43.04	48.27	3.17
	60	32.00	26.80	29.69	2.04	44.52	38.56	41.11	2.51
					Arugula				
Yield (t ha^{-1})	100	53.86	45.63	48.24	3.34	54.00	48.67	51.15	2.08
	80	38.59	32.69	34.79	2.52	34.56	28.80	32.83	2.44
	60	24.48	22.32	23.64	0.93	28.66	25.06	27.68	1.49

Max: maximum; Min: minimum; $\bar{x}$: mean; σ: standard deviation.

studied crops, resulting in a greater yield reduction under increased water deficit. This effect may occur even in irrigated systems when irrigation is poorly managed, or in regions with low rainfall regimes. Therefore, continuous crop monitoring is important for detecting water deficit conditions, as obtaining data on plant water status enables rapid corrective actions, such as timely irrigation, to prevent yield losses. CWSI values equal to or near zero indicate that the plants are under favorable water conditions, with adequate transpiration and photosynthesis rates, contributing to enhanced growth and higher yield, as observed under the 100 % ETc irrigation condition.

Fig. 6 shows the correlation between CWSI and lettuce yield (Fig. 6A) and arugula yield (Fig. 6B), as well as between ΔT and lettuce yield (Fig. 6C) and arugula yield (Fig. 6D), considering both cultivation cycles. An inverse relationship was observed in both crops, indicating that increases in CWSI or ΔT values were associated with decreases in leafy vegetables yield. The coefficients of determination (R^2) for lettuce were 0.71 and 0.75 for CWSI and ΔT, respectively, while for arugula they were 0.82 and 0.79, respectively. It is worth noting that the models developed using both thermal indices demonstrated similar performance in predicting the yield of leafy vegetables, suggesting that both CWSI and ΔT are reliable indicators for this purpose.

Regarding the prediction of leafy vegetables yield based on models derived from the correlation between thermal indices and observed yield (Fig. 7), the predicted values closely matched the observed values for both lettuce (Fig. 7A and 7C) and arugula (Fig. 7B and 7D). This agreement is evidenced by the dispersion of data points around the 1:1 reference line. Overall, arugula showed less dispersion compared to lettuce for both thermal indices.

Predicting the yield of leafy vegetables such as lettuce and arugula using the developed models enables the use of remote sensing tools with infrared sensors to estimate crop yield accurately and in real time, even before harvest. By monitoring thermal indices throughout the crop

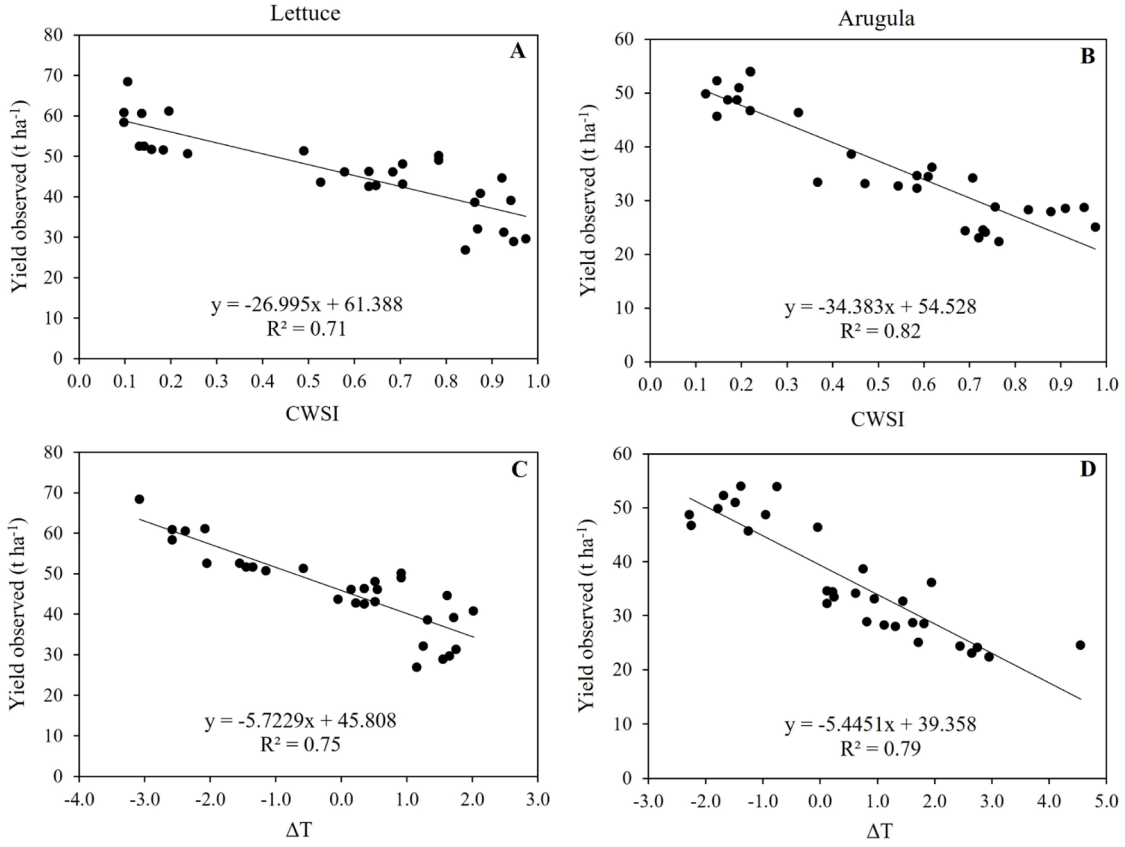

Fig. 6. Correlation analysis between Crop Water Stress Index (CWSI) and normalized temperature difference (ΔT) values with leafy vegetables yield observed considering the two crop cycles. A) and C) Lettuce; and B) and D) Arugula.

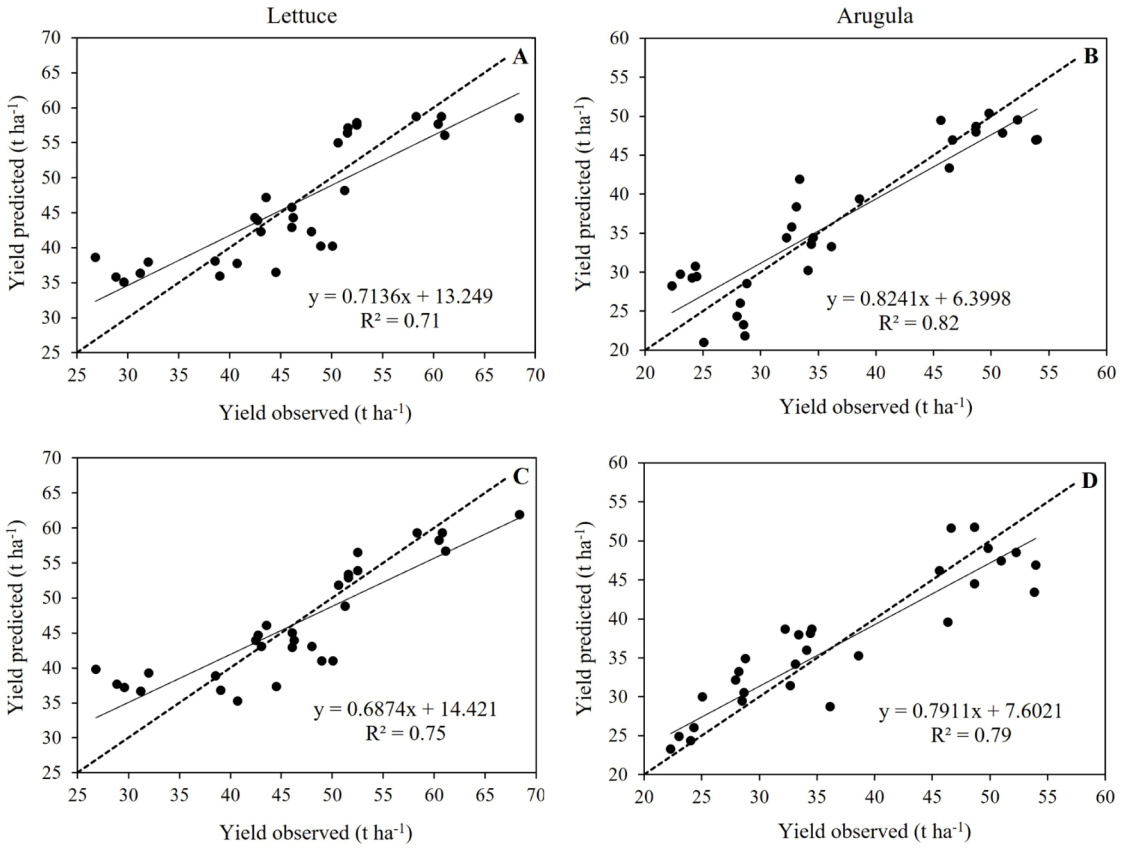

Fig. 7. Prediction of leafy vegetables yield using models derived from the correlation analysis of the two crop cycles. A) and C) Lettuce; and B) and D) Arugula.

cycle, farmers can anticipate how the intensity of a possible water stress is affecting plant development and adjust irrigation management accordingly before yield losses become irreversible. This is particularly important for short-cycle crops like leafy vegetables, where just a few days of water stress may result in significant productivity losses, leaving limited time for corrective measures.

In addition to the crop water status, soil water content can also be used for irrigation management. Soil water content can be expressed as matric potential, indicating the availability of water in the soil for plant uptake. Although these factors are interrelated, water dynamics within the soil–plant–atmosphere continuum must be analyzed individually for effective irrigation management. While crop water status allows for identifying the proper timing for irrigation, knowing the soil water content enables the planning of irrigation events in terms of both timing and the amount of water to be applied [30].

3.4. *Thermal parameters for predicting soil water content*

Fig. 8 presents the average values of soil water potential on the day of thermal image acquisition, considering both cultivation cycles. It can be observed that, for the same vegetable crop, the soil water potential values are similar across the two cultivation cycles.

Analyzing the soil water potential for lettuce (Fig. 8A), in the first cycle, the values were −13.50, −26.50, and −50.50 kPa, while in the second cycle, they were −15.50, −28.20, and −47.00 kPa, resulting in average values of −14.50, −27.35, and −48.75 kPa for the 100, 80, and

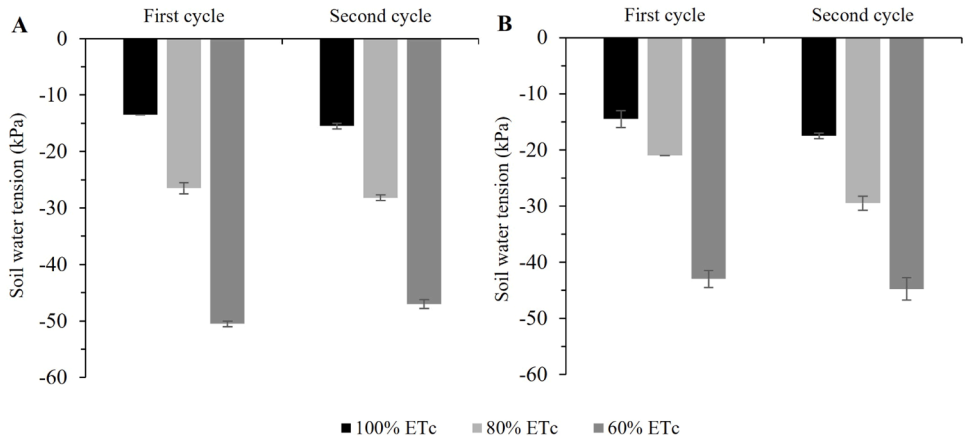

Fig. 8. Characterization of the average soil water potential (-kPa) on the day of thermal image acquisition of leafy vegetables for the two crop cycles. A) Lettuce, and B) Arugula.

60 % ETc treatments, respectively. For arugula (Fig. 8B), in the first cycle, the values were −14.50, −21.00, and −43.00 kPa, and in the second cycle, they were −17.50, −29.50, and −44.80 kPa, resulting in average values of −16.00, −25.25, and −43.90 kPa for the 100, 80, and 60 % ETc treatments, respectively. Regarding the soil water content equivalent to the average soil water potential values, they were 0.369, 0.355, and 0.342 $m^3 m^{-3}$ for lettuce, and 0.367, 0.356, and 0.344 $m^3 m^{-3}$ for arugula, for the 100, 80, and 60 % ETc treatments, respectively.

In both crops, the lowest soil water potential values were observed in the treatment where plants were subjected to the greatest water deficit condition (60 % of ETc), while the highest values were recorded under the treatment with optimal water replacement level (100 % of ETc), indicating drier and wetter soil conditions, respectively. For leafy vegetables in general, including lettuce and arugula, the soil water potential threshold is around −20 kPa, which may vary between −10 and −20 kPa depending on the soil's water retention capacity and the phenological stage of the crop [45]. In coarse-textured soils (sandy), which typically have lower water retention capacity, and during more sensitive growth stages, such as the initial establishment phase, it is recommended that the soil water potential not fall below −10 kPa to avoid water stress. As observed, only in the 100 % ETc treatment were the soil water potential values above the threshold (−20 kPa) for leafy vegetables, confirming that the plants under the other treatments were indeed exposed to water deficit conditions.

Fig. 9 presents the correlation analysis between thermal parameters and soil water content, considering both crop cycles of the leafy vegetables. It was found that both the CWSI (Fig. 9A) and ΔT (Fig. 9B) exhibited a strong correlation with soil water content, with R^2 values of 0.92 and 0.73, respectively. These relationships were inversely proportional, meaning that as CWSI and ΔT increased, soil water content decreased. Specifically, for each 0.1 unit increase in CWSI, there was a 3.45 % reduction in soil water content, and for each 0.1 unit increase in ΔT, soil water content decreased by 0.57 %. Among the two thermal parameters, CWSI demonstrated superior performance in predicting soil water content compared to ΔT, indicating its greater potential as a tool for supporting irrigation management.

Considering the soil water content values predicted by the models (Fig. 10), it was observed that the predicted values were close to the observed ones. However, the model developed using CWSI (Fig. 10A) showed less data dispersion around the reference line, resulting in more accurate predictions compared to the model developed using ΔT (Fig. 10B). Although ΔT demonstrated lower accuracy than CWSI, it still achieved satisfactory results and can be considered a viable alternative for irrigation management.

Notably, in the model based on CWSI, more dispersion was observed for intermediate values (80 % of ETc), which may be related to the coexistence of water-filled and air-filled soil pores under this condition, leading to greater variability in canopy temperature compared to the other treatments. Under the 100 % ETc condition, most pores would be filled with water, resulting in reduced and more stable canopy temperatures. Conversely, under the 60 % ETc condition, most pores would lack water, causing increased temperatures but with lower variation, since the soil pores are more uniformly dry.

The CWSI, obtained based on leaf temperature, not only enables the assessment of plant water stress levels but also shows strong potential for predicting soil water content, as the morphophysiological responses of plants are also associated with the management practices to which they are subjected. In this context, the lack of water in the soil to meet crop demand can lead to several physiological disturbances in the plant and impair essential cellular functions [61]. At any sign of water stress emitted by the plant, leaf temperature changes due to metabolic processes associated with osmoregulation, cellular respiration, and variations in photosynthetic rate [20,62].

It was observed that the values associated with each treatment were concentrated within specific ranges of CWSI and volumetric soil water content, demonstrating that the model developed for soil moisture prediction can be applied both when plants are subjected to different water availability conditions, within the 60 % to 100 % ETc range, and for monitoring soil water content throughout the crop cycle. In this case, the behavior is consistent with the different irrigation levels analyzed in this study, reflecting the soil transitioning from field capacity (100 %) to a condition where the current moisture corresponds to 60 % of the available soil water. The use of the model to predict soil water content under irrigation levels below 60 % of ETc is not recommended, as this represents the lower limit analyzed in this study. Furthermore, it reflects a condition of severe stress for leafy vegetable cultivation, and it is not advisable for soil water content to fall below this threshold.

Based on the developed models and the critical soil water potential for leafy vegetables (−20 kPa), it is recommended, especially for lettuce and arugula, that CWSI and ΔT values above 0.35 and −0.96 °C, respectively, be considered as critical thresholds to prevent the crops from entering water deficit stress. These thresholds represent the limit at which irrigation should be applied. In the case of ΔT, its negative threshold is justified by the plant's early expression of reduced leaf turgor in response to approaching the critical soil moisture level, as leafy vegetables are highly sensitive to water stress. In this context, when ΔT reaches −0.96 °C, the plant has not yet entered into a critical stress condition. However, if irrigation is not applied near this point, the leaf temperature will likely equal or exceed air temperature, reaching critical stress levels due to water deficiency, which may result in yield losses.

The CWSI threshold value identified in this study is consistent with those reported in the literature for other crops. Kumari [29] emphasize that for wheat, irrigation should be triggered when the CWSI reaches

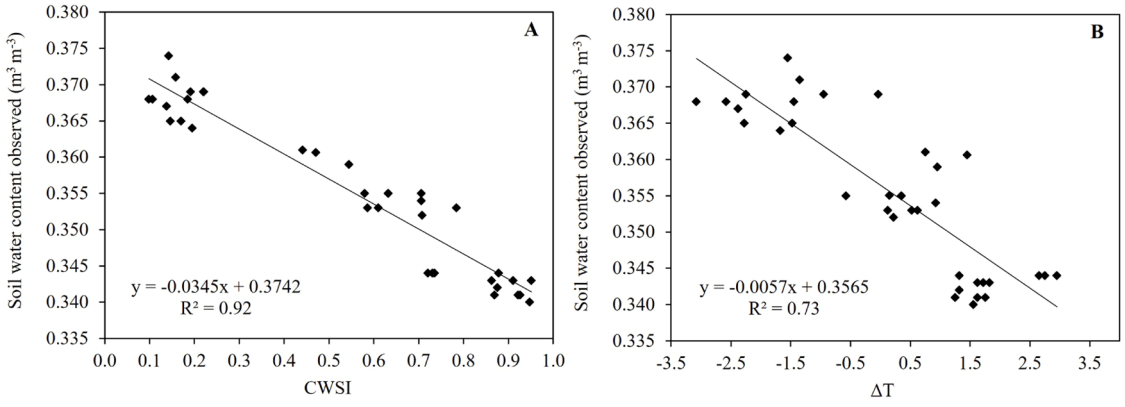

Fig. 9. Correlation analysis between Crop Water Stress Index (CWSI) (A) and normalized temperature difference (ΔT) (B) values with soil water content, considering the two crop cycles of leafy vegetables.

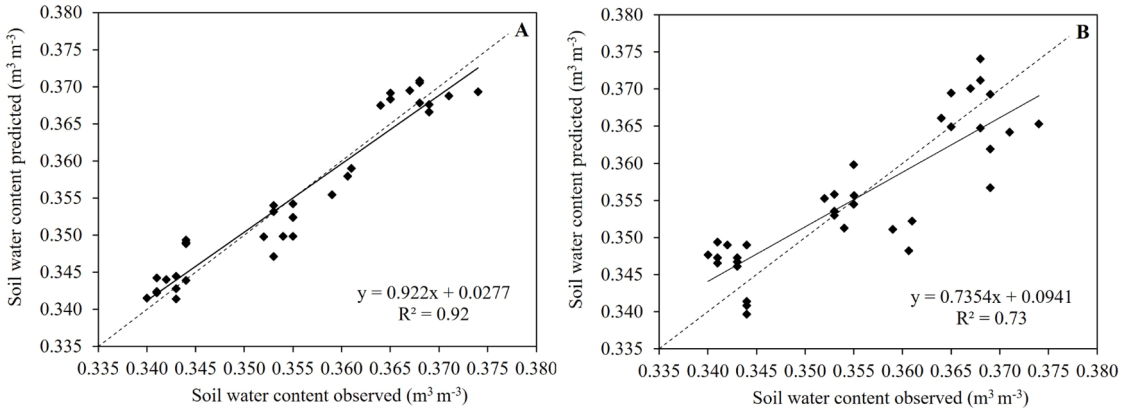

Fig. 10. Prediction of soil water content using models derived from the correlation analysis of Crop Water Stress Index (CWSI) (A) and normalized temperature difference (ΔT) (B), considering the two crop cycles of leafy vegetables.

values equal to or greater than 0.35, to avoid stress and ensure high yields. Similarly, Ma [20] demonstrated that CWSI is a useful tool for decision-making in the irrigation management of winter wheat, allowing for stratification according to phenological stages. Their recommendations suggest that CWSI values should be maintained within the ranges of 0.26–0.38, 0.27–0.32, and 0.30–0.36 during the stem elongation, flowering, and grain filling stages, respectively.

3.5. Assessment of the predictive models

Table 8 presents the values of the statistical parameters used to evaluate the yield prediction models for lettuce and arugula. Regarding the yield prediction models based on the CWSI, the RMSE values were 5.399 and 4.319 t ha^{-1}, and the MAE values were 4.515 and 3.575 t ha^{-1} for lettuce and arugula, respectively, indicating low prediction errors. Considering the NSE and the agreement index "d", which assess model efficiency, the models were classified as acceptable, with NSE values of 0.714 and 0.824, and "d" values of 0.904 and 0.948 for lettuce and arugula, respectively. The correlation strength, evaluated by the Pearson correlation coefficient "r", was classified as very high (r = 0.845) for lettuce and nearly perfect (r = 0.908) for arugula. According to the confidence index "c", the yield prediction model for lettuce showed very good performance, while the model for arugula showed excellent performance, with values of 0.764 and 0.861, respectively.

The models based on ΔT showed RMSE values of 5.077 and 4.707 t ha^{-1}, and MAE values of 3.988 and 3.895 t ha^{-1} for lettuce and arugula, respectively, also indicating low prediction errors. Considering the NSE and the "d" index, these models were also classified as acceptable, with NSE values of 0.747 and 0.791, and "d" index values of 0.905 and 0.944 for lettuce and arugula, respectively. The correlation strength, assessed by Pearson's r, was very high (r = 0.866) for lettuce and nearly perfect (r = 0.889) for arugula. According to the confidence index "c", both models were classified as very good, with values of 0.784 and 0.839, respectively.

Table 9 presents the values of the statistical parameters used to evaluate the soil water content prediction model in the cultivation of leafy vegetables. For the model based on CWSI, low prediction errors were observed, with an RMSE of 0.00301 $m^3\ m^{-3}$ and an MAE of 0.00258 $m^3\ m^{-3}$. In terms of efficiency, the model was classified as acceptable, with NSE and Willmott's index "d" values of 0.921 and 0.979, respectively. Regarding the degree of correlation, evaluated by the Pearson correlation coefficient "r," it was classified as almost perfect (r = 0.959). As for the confidence index "c," the prediction model for soil water content in leafy vegetable cultivation showed optimal performance, with a value of 0.939.

Low prediction errors were also observed for the model based on ΔT, although these were higher than those of the model based on CWSI. The RMSE value was 0.00554 $m^3\ m^{-3}$, and the MAE value was 0.00453 $m^3\ m^{-3}$. Considering efficiency, the model was classified as acceptable, with NSE and Willmott's index "d" values of 0.733 and 0.921, respectively. Regarding the degree of correlation, evaluated by the Pearson correlation coefficient "r," it was classified as almost perfect (r = 0.854). As for the confidence index "c" the soil water content prediction model for leafy vegetable cultivation showed very good performance, with a value of 0.787.

4. Conclusions

The models developed from thermal images captured by infrared radiation cameras showed good performance in predicting the yield of lettuce and arugula, as well as in predicting soil water content in leafy vegetable cultivation under protected environment. The thermal parameters used in this study, CWSI and ΔT, contributed to characterize the water deficit in leafy vegetables, distinguishing the different irrigation levels to which the plants were subjected. Considering both cultivation cycles, under conditions of 100, 80, and 60 % of ETc, respectively, the average CWSI values for lettuce were 0.15, 0.65, and 0.88, and for arugula were 0.20, 0.57, and 0.82, while the average ΔT

Table 8
Statistical parameters used to evaluate the yield prediction models for lettuce and arugula.

Crop	RMSE	MAE	NSE	d	r	Index "c"	
						Value	Performance
Crop Water Stress Index (CWSI)							
Lettuce	5.399	4.515	0.714	0.904	0.845	0.764	Very good
Arugula	4.319	3.575	0.824	0.948	0.908	0.861	Great
Normalized temperature difference (ΔT)							
Lettuce	5.077	3.988	0.747	0.905	0.866	0.784	Very good
Arugula	4.707	3.895	0.791	0.944	0.889	0.839	Very good

RMSE: root mean square error; MAE: mean absolute error; NSE: Nash–Sutcliffe efficiency; d: Willmott's index of agreement; r: Pearson's correlation coefficient; and "c": confidence index.

Table 9
Statistical parameters used to evaluate the soil water content prediction models in leafy vegetable cultivation.

Crop	RMSE	MAE	NSE	d	r	Index "c"	
						Value	Performance
Crop Water Stress Index (CWSI)							
Leafy vegetables	0.00301	0.00258	0.921	0.979	0.959	0.939	Great
Normalized temperature difference (ΔT)							
Leafy vegetables	0.00554	0.00453	0.733	0.921	0.854	0.787	Very good

RMSE: root mean square error; MAE: mean absolute error; NSE: Nash–Sutcliffe efficiency; d: Willmott's index of agreement; r: Pearson's correlation coefficient; and "c": confidence index.

values for lettuce were −2.03, 0.37, and 1.43 °C, and for arugula were −1.38, 0.77, and 2.30 °C.

The yield prediction models for lettuce were classified as very good when considering both CWSI and ΔT. For arugula, the models were classified as excellent based on CWSI and very good based on ΔT. Since the models based on CWSI and ΔT showed similar results, both thermal indices can be used for predicting the yield of these two crops.

The soil water content prediction models were classified as excellent when based on CWSI and very good when based on ΔT. For this purpose, the use of CWSI is recommended due to its better performance compared to ΔT. Based on the generated models, it is suggested that for leafy vegetables, especially lettuce and arugula, CWSI and ΔT values of 0.35 and −0.96 °C, respectively, constitute critical thresholds for water deficit stress.

The use of thermal imaging demonstrated great potential in developing prediction models. The results obtained in this study may support decision-making in irrigation management and in the early identification of water stress damage affecting the yield of leafy vegetables. For future research, it is recommended to evaluate the performance of CWSI and ΔT indices in other leafy vegetables. It is suggested to consider stratification by phenological stages and a wider range of water deficit levels, as well as to evaluate in open-field cultivation environments.

Funding sources

This research received no external funding.

Ethics in publishing statement

All authors agree that:

This research presents an accurate account of the work performed, all data presented are accurate and methodologies detailed enough to permit others to replicate the work.

This manuscript represents entirely original works and or if work and/or words of others have been used, that this has been appropriately cited or quoted and permission has been obtained where necessary.

This material has not been published in whole or in part elsewhere.

The manuscript is not currently being considered for publication in another journal.

That generative AI and AI-assisted technologies have not been utilized in the writing process or if used, disclosed in the manuscript the use of AI and AI-assisted technologies and a statement will appear in the published work.

That generative AI and AI-assisted technologies have not been used to create or alter images unless specifically used as part of the research design where such use must be described in a reproducible manner in the methods section.

All authors have been personally and actively involved in substantive work leading to the manuscript and will hold themselves jointly and individually responsible for its content.

CRediT authorship contribution statement

Vinícius Villa e Vila: Writing – review & editing, Writing – original draft, Visualization, Validation, Resources, Methodology, Investigation, Formal analysis, Data curation, Conceptualization. **Silas Alves Souza:** Writing – review & editing, Writing – original draft, Visualization, Validation, Resources, Methodology, Investigation, Formal analysis, Data curation, Conceptualization. **Fernando Campos Mendonça:** Writing – review & editing, Visualization, Validation, Supervision, Resources. **Tamara Maria Gomes:** Writing – review & editing, Visualization, Validation, Resources, Investigation. **Peterson Ricardo Fiorio:** Writing – review & editing, Visualization, Validation, Resources, Investigation. **Patricia Angélica Alves Marques:** Writing – review & editing, Visualization, Validation, Supervision, Resources, Project administration, Conceptualization.

Declaration of competing interest

The authors declare that they have no known competing financial interests or personal relationships that could have appeared to influence the work reported in this paper.

Acknowledgements

We thank the Coordination for the Improvement of Higher Education Personnel (CAPES), finance code 001, and the National Council for Scientific and Technological Development (CNPq – Case number 156142/2021–0) for scholarships. We also thank the Luiz de Queiroz Agricultural Studies Foundation (FEALQ) for supporting the research.

Data availability

Data will be made available on request.

References

[1] P. Berry, J. Ramirez-Villegas, H. Bramley, M.A. Mgonja, S.M. Samarendu Mohanty, Regional impacts of climate change on agriculture and the role of adaptation, Plant Genet Resour. Clim. Change (2013) 78–97, https://doi.org/10.1079/9781780641973.0078.

[2] R. Joshi, S.L. Singla-Pareek, A. Pareek, Engineering abiotic stress response in plants for biomass production, J. Biol. Chem. 293 (2018) 5035–5043, https://doi.org/10.1074/jbc.TM117.000232.

[3] S. Das, J. Christopher, A. Apan, M.R. Choudhury, S. Chapman, N.W. Menzies, Y. P. Dang, Evaluation of water status of wheat genotypes to aid prediction of yield on sodic soils using UAV-thermal imaging and machine learning, Agric. Meteorol. 307 (2021) 108447, https://doi.org/10.1016/j.agrformet.2021.108477.

[4] V. Villa e Vila, P.A.A. Marques, T.M. Gomes, A.F. Nunes, V.G. Montenegro, G. S. Wenneck, L.B. Franco, Deficit irrigation with silicon application as strategy to increase yield, photosynthesis and water productivity in lettuce crops, Plants 13 (2024) 1029, https://doi.org/10.3390/plants13071029.

[5] N. Akter, M. Rafiqul Islam, Heat stress effects and management in wheat. A review, Agron. Sustain. Dev. 37 (2017) 37, https://doi.org/10.1007/s13593-017-0443-9.

[6] M. Knez, K. Mattas, M. Gurinovic, A. Gkotzamani, A. Koukounaras, Revealing the power of green leafy vegetables: cultivating diversity for health, environmental benefits, and sustainability, Glob. Food Sec. 43 (2024) 100816, https://doi.org/10.1016/j.gfs.2024.100816.

[7] M.W. Rasheed, J. Tang, A. Sarwar, S. Shah, N. Saddique, M.U. Khan, M. Imran Khan, S. Nawaz, R.R. Shamshiri, M. Aziz, Soil moisture measuring techniques and factors affecting the moisture dynamics: a comprehensive review, Sustainability 14 (2022) 11538, https://doi.org/10.3390/su141811538.

[8] Z. Zhou, Y. Majeed, G. Diverres Naranjo, E.M.T. Gambacorta, Assessment for crop water stress with infrared thermal imagery in precision agriculture: a review and

future prospects for deep learning applications, Comput. Electron. Agric. 182 (2021) 106019, https://doi.org/10.1016/j.compag.2021.106019.
[9] S. Elsayed, M. Elhoweity, H.H. Ibrahim, Y.H. Dewir, H.M. Migdadi, U. Schmidhalter, Thermal imaging and passive reflectance sensing to estimate the water status and grain yield of wheat under different irrigation regimes, Agric. Water. Manag. 189 (2017) 98–110, https://doi.org/10.1016/j.agwat.2017.05.001.
[10] B. Zhang, J. Huang, T. Dai, S. Jing, Y. Hua, Q. Zhang, H. Liu, Y. Wu, Z. Zhang, J. Chen, Assessing accuracy of crop water stress inversion of soil water content all day long, Precis. Agric. 25 (2024) 1894–1914, https://doi.org/10.1007/s11119-024-10143-y.
[11] L. Zhang, Y. Niu, H. Zhang, W. Han, G. Li, J. Tang, X. Peng, Maize canopy temperature extracted from UAV thermal and RGB imagery and its application in water stress monitoring, Front. Plant Sci. 10 (2019) 1270, https://doi.org/10.3389/fpls.2019.01270.
[12] S. Das, J. Christopher, A. Apan, M. Roy Choudhury, S. Chapman, N.W. Menzies, Y. P. Dang, UAV-thermal imaging and agglomerative hierarchical clustering techniques to evaluate and rank physiological performance of wheat genotypes on sodic soil, ISPRS. J. Photogramm. Remote Sens. 173 (2021) 221–237, https://doi.org/10.1016/j.isprsjprs.2021.01.014.
[13] G. Fevgas, T. Lagkas, P. Papadopoulos, P. Sarigiannidis, V. Argyriou, Integrating thermal infrared and RGB imaging for early detection of water stress in lettuces with comparative analysis of IoT sensors, Smart Agr. Technol. 11 (2025) 100881, https://doi.org/10.1016/j.atech.2025.100881.
[14] J. Kang, X. Hao, H. Zhou, R. Ding, An integrated strategy for improving water use efficiency by understanding physiological mechanisms of crops responding to water deficit: present and prospect, Agric. Water. Manag. 255 (2021) 107008, https://doi.org/10.1016/j.agwat.2021.107008.
[15] V. Parkash, S. Singh, S.K. Deb, G.L. Ritchie, R.W. Wallace, Effect of deficit irrigation on physiology, plant growth, and fruit yield of cucumber cultivars, Plant Stress 1 (2021) 100004, https://doi.org/10.1016/j.stress.2021.100004.
[16] C. Wang, K. Zhu, Y.Y. Bai, C.Y. Li, M. Li, Y. Sun, Response of stomatal conductance to plant water stress in buffalograss seed production: observation with UAV thermal infrared imagery, Agric. Water. Manag. 292 (2024) 108661, https://doi.org/10.1016/j.agwat.2023.108661.
[17] H.S. Ndlovu, J. Odindi, M. Sibanda, O. Mutanga, Multi-temporal analysis of taro crop water stress using high-resolution thermal and multispectral proximal sensing for improved resilience of smallholder farming systems, Smart Agr. Technol. 12 (2025) 101337, https://doi.org/10.1016/j.atech.2025.101337.
[18] R. Ludovisi, F. Tauro, R. Salvati, S. Khoury, G.S. Mugnozza, A. Harfouche, Uav-based thermal imaging for high-throughput field phenotyping of black poplar response to drought, Front. Plant Sci. 8 (2017) 1681, https://doi.org/10.3389/fpls.2017.01681.
[19] M. Pineda, M. Barón, M.L. Pérez-Bueno, Thermal imaging for plant stress detection and phenotyping, Remote Sens. 13 (2021) 68, https://doi.org/10.3390/rs13010068.
[20] S. Ma, S. Liu, Z. Gao, X. Wang, S. Ma, S. Wang, Water deficit diagnosis of winter wheat based on thermal infrared imaging, Plants 13 (2024) 361, https://doi.org/10.3390/plants13030361.
[21] C. Pradawet, N. Khongdee, W. Pansak, W. Spreer, T. Hilger, G. Cadisch, Thermal imaging for assessment of maize water stress and yield prediction under drought conditions, J. Agron. Crop. Sci. 209 (2023) 56–70, https://doi.org/10.1111/jac.12582.
[22] E. Bijanzadeh, S.M. Moosavi, F. Bahadori, Quantifying water stress of safflower (*Carthamus tinctorius* L.) cultivars by crop water stress index under different irrigation regimes, Heliyon 8 (2022) e09010, https://doi.org/10.1016/j.heliyon.2022.e09010.
[23] H. Dong, J. Dong, S. Sun, T. Bai, D. Zhao, Y. Yin, X. Shen, Y. Wang, Z. Zhang, Y. Wang, Crop water stress detection based on UAV remote sensing systems, Agric. Water. Manag. 303 (2024) 109059, https://doi.org/10.1016/j.agwat.2024.109059.
[24] S.B. Idso, R.D. Jackson, P.J. Pinter, R.J. Reginato, J.L. Hatfield, Normalizing the stress-degree-day parameter for environmental variability, Agric. Meteorol. 24 (1981) 45–55, https://doi.org/10.1016/0002-1571(81)90032-7.
[25] R.D. Jackson, S.B. Idso, R.J. Reginato, P.J. Pinter, Canopy temperature as a crop water stress indicator, Water Resour. Res. 17 (1981) 1133–1138, https://doi.org/10.1029/WR017i004p01133.
[26] H. Zhang, L.H. Manh, D.H. Ha, A. Andales, S. Wang, Prototype web-based platform for the calculation of crop water stress index for irrigation scheduling – An application note, Comput. Electron. Agric. 230 (2025) 109870, https://doi.org/10.1016/j.compag.2024.109870.
[27] S. Pappalardo, S. Consoli, G. Longo-Minnolo, D. Vanella, D. Longo, S. Guarrera, A. D'Emilio, J.M. Ramírez-Cuesta, Performance evaluation of a low-cost thermal camera for citrus water status estimation, Agric. Water. Manag. 288 (2023) 108489, https://doi.org/10.1016/j.agwat.2023.108489.
[28] A.P. Nugroho, A. Wiratmoko, D. Nugraha, S. Markumningsih, L. Sutiarso, M.A. F. Falah, T. Okayasu, Development of a low-cost thermal imaging system for water stress monitoring in indoor farming, Smart Agr. Technol. 11 (2025) 101048, https://doi.org/10.1016/j.atech.2025.101048.
[29] A. Kumari, D.K. Singh, A. Sarangi, M. Hasan, V.K. Sehgal, Optimizing wheat supplementary irrigation: integrating soil stress and crop water stress index for smart scheduling, Agric. Water. Manag. 305 (2024) 109104, https://doi.org/10.1016/j.agwat.2024.109104.
[30] A. Morales-Santos, R. Nolz, Assessment of canopy temperature-based water stress indices for irrigated and rainfed soybeans under subhumid conditions, Agric. Water. Manag. 279 (2023) 108214, https://doi.org/10.1016/j.agwat.2023.108214.
[31] V. Gonzalez-Dugo, P.J. Zarco-Tejada, E. Fereres, Applicability and limitations of using the crop water stress index as an indicator of water deficits in citrus orchards, Agric. Meteorol. 198–199 (2014) 94–104, https://doi.org/10.1016/j.agrformet.2014.08.003.
[32] B.A. King, K.C. Shellie, D.D. Tarkalson, A.D. Levin, V. Sharma, D.L. Bjorneberg, Data-driven models for canopy temperature-based irrigation scheduling, Trans. ASABE 63 (2020) 1579–1592, https://doi.org/10.13031/TRANS.13901).
[33] S. Gutiérrez, J. Fernández-Novales, M.P. Diago, R. Iñiguez, J. Tardaguila, Assessing and mapping vineyard water status using a ground mobile thermal imaging platform, Irrig. Sci. 39 (2021) 457–468, https://doi.org/10.1007/s00271-021-00735-1.
[34] A. Peeters, Y. Cohen, I. Bahat, N. Ohana-Levi, E. Goldshtein, Y. Netzer, T. R Tenreiro, V. Alchanatis, A. Ben-Gal, A spatial machine-learning model for predicting crop water stress index for precision irrigation of vineyards, Comput. Electron. Agric. 227 (2024) 109578, https://doi.org/10.1016/j.compag.2024.109578.
[35] B.A. King, D.D. Tarkalson, V. Sharma, D.L. Bjorneberg, Thermal crop water stress index base line temperatures for sugarbeet in arid western U.S, Agric. Water. Manag. 243 (2021) 106459, https://doi.org/10.1016/j.agwat.2020.106459.
[36] C.A. Alvares, J.L. Stape, P.C. Sentelhas, J.L. de Moraes Gonçalves, G. Sparovek, Köppen's climate classification map for Brazil, Meteorol. Z. 22 (2013) 711–728, https://doi.org/10.1127/0941-2948/2013/0507.
[37] Dias, S.H.B., 2018. Evapotranspiração de referência para projeto de irrigação no Brasil utilizando o produto MOD16.
[38] H.G.D. Santos, P.K.T. Jacomine, L.H.C.D. Anjos, V.A.D. Oliveira, J.F. Lumbreras, M.R. Coelho, J.A.D. Almeida, J.C.D. Araujo Filho, J.B.D. Oliveira, T.J.F. Cunha, Sistema Brasileiro de Ciência do Solo, 355, Embrapa Solos, 2018.
[39] B. Van Raij, H. Cantarella, J.A. Quaggio, A.M.C. Furlani, Recomendações De Adubação e Calagem Para o Estado de São Paulo, Instituto Agronômico de Campinas, Campinas-SP, Brasil, 1997.
[40] R.G. Allen, L.S. Pereira, D. Raes, M. Smith, Crop evapotranspiration: Guidelines For Computing Crop Water Requirements (FAO. Irrigation and Drainage Paper, 56), FAO, Rome, Italy, 1998.
[41] O.A. Camargo, A.C. Moniz, J.A. Jorge, J.M.A.S. Valadares, Métodos de análise química, mineralógica e física de solo do instituto agronômico de campinas, Campinas, Instituto Agronômico (1986) 94. Boletim técnico, 106.
[42] M.T. Van Genuchten, A closed-form equation for predicting the hydraulic conductivity of unsaturated soils, Soil. Sci. Soc. Am. J. 44 (1980) 892–898, https://doi.org/10.2136/sssaj1980.03615995004400050002x.
[43] S.B. Idso, Non-water-stressed baselines: a key to measuring and interpreting plant water stress, Agric. Meteorol. 27 (1982) 59–70, https://doi.org/10.1016/0002-1571(82)90020-6.
[44] H.G. Jones, Use of infrared thermography for monitoring stomatal closure in the field: application to grapevine, J. Exp. Bot. 53 (2002) 2249–2260, https://doi.org/10.1093/jxb/erf083.
[45] W.A. Marouelli, Tensiômetros Para o Controle de Irrigação em Hortaliças, Empresa Brasileira de Pesquisa Agropecuária, Brasília-DF, 2008.
[46] D.N. Moriasi, J.G. Arnold, M.W. Van Liew, R.L. Bingner, R.D. Harmel, T.L. Veith, Model evaluation guidelines for systematic quantification of accuracy in watershed simulations, Trans. ASABE 50 (2007) 885–900, https://doi.org/10.13031/2013.23153.
[47] C.J. Willmott, S.G. Ackleson, R.E. Davis, J.J. Feddema, K.M. Klink, D.R. Legates, J. O'Donnell, C.M. Rowe, Statistics for the evaluation and comparison of models, J. Geophys. Res. Oceans 90 (1985) 8995–9005, https://doi.org/10.1029/JC090IC05P08995.
[48] W.G. Hopkins, A New View of Statistics [WWW Document], Internet Society for Sport Science, 2000. URL, http://www.sportsci.org/resource/stats/. accessed 4.10.25.
[49] A.P.D. Camargo, P.C. Sentelhas, Avaliação do desempenho de diferentes métodos de estimativa da evapotranspiração potencial no Estado de São Paulo, Brasil, Rev. Bras. Agrometeorol. 5 (1997) 89–97.
[50] M.B. Bisbis, N. Gruda, M. Blanke, Potential impacts of climate change on vegetable production and product quality – a review, J. Clean. Prod. 170 (2018) 1602–1620, https://doi.org/10.1016/j.jclepro.2017.09.224.
[51] J. Dong, N. Gruda, X. Li, Y. Tang, P. Zhang, Z. Duan, Sustainable vegetable production under changing climate: the impact of elevated CO_2 on yield of vegetables and the interactions with environments-a review, J. Clean. Prod. 253 (2020) 119920, https://doi.org/10.1016/j.jclepro.2019.119920.
[52] A. Alvino, G. Barbieri, Vegetables of temperate climates: leafy vegetables. Encyclopedia of Food and Health, Elsevier Inc., 2015, pp. 393–400, https://doi.org/10.1016/B978-0-12-384947-2.00712-1.
[53] L. Carotti, L. Graamans, F. Puksic, M. Butturini, E. Meinen, E. Heuvelink, C. Stanghellini, Plant factories are heating up: hunting for the best combination of light intensity, air temperature and root-zone temperature in lettuce production, Front. Plant Sci. 11 (2021) 592171, https://doi.org/10.3389/fpls.2020.592171.
[54] M. Giordano, S.A. Petropoulos, Y. Rouphael, Response and defence mechanisms of vegetable crops against drought, heat and salinity stress, Agriculture 11 (2021) 463, https://doi.org/10.3390/agriculture11050463.
[55] F. Saeed, U.K. Chaudhry, A. Raza, S. Charagh, A. Bakhsh, A. Bohra, S. Ali, A. Chitikineni, Y. Saeed, R.G.F. Visser, K.H.M. Siddique, R.K. Varshney, Developing future heat-resilient vegetable crops, Funct. Integr. Genom. 23 (2023) 47, https://doi.org/10.1007/s10142-023-00967-8.
[56] D.K. Vishwakarma, K. Pandey, A. Kaur, N.L. Kushwaha, R. Kumar, R. Ali, A. Elbeltagi, A. Kuriqi, Methods to estimate evapotranspiration in humid and subtropical climate conditions, Agric. Water. Manag. 261 (2022) 107378, https://doi.org/10.1016/j.agwat.2021.107378.

[57] W. Ishaque, R. Osman, B.S. Hafiza, S. Malghani, B. Zhao, M. Xu, S.T. Ata-Ul-Karim, Quantifying the impacts of climate change on wheat phenology, yield, and evapotranspiration under irrigated and rainfed conditions, Agric. Water. Manag. 275 (2023) 108017, https://doi.org/10.1016/j.agwat.2022.108017.

[58] W. Shtai, D. Asensio, A.E. Kadison, M. Schwarz, B. Raifer, C. Andreotti, A. Hammerle, D. Zanotelli, F. Haas, G. Niedrist, G. Wohlfahrt, M. Tagliavini, Soil water availability modulates the response of grapevine leaf gas exchange and PSII traits to a simulated heat wave, Plant Soil. 501 (2024) 537–554, https://doi.org/10.1007/s11104-024-06536-7.

[59] K. Jumrani, V.S. Bhatia, S. Hussain, S. Kataria, X. Yang, M. Brestic, Effect of shading on leaf anatomical structure, photosynthesis characteristics and chlorophyll fluorescence of soybean (*Glycine* max), J. Agron. Crop. Sci. 210 (2024) e12783, https://doi.org/10.1111/jac.12783.

[60] C. Ru, X. Hu, W. Wang, H. Yan, Impact of nitrogen on photosynthesis, remobilization, yield, and efficiency in winter wheat under heat and drought stress, Agric. Water. Manag. 302 (2024) 109013, https://doi.org/10.1016/j.agwat.2024.109013.

[61] I. Medyouni, R. Zouaoui, E. Rubio, S. Serino, H.B. Ahmed, N. Bertin, Effects of water deficit on leaves and fruit quality during the development period in tomato plant, Food Sci. Nutr. 9 (2021) 1949–1960, https://doi.org/10.1002/fsn3.2160.

[62] V. Blanco, N. Willsea, T. Campbell, O. Howe, L. Kalcsits, Combining thermal imaging and soil water content sensors to assess tree water status in pear trees, Front. Plant Sci. 14 (2023) 1197437, https://doi.org/10.3389/fpls.2023.1197437.